CRYSTAL GROWTH & DESIGN

Subscriber access provided by - Access paid by the | UCSB Libraries

Modulation of nuclearity by Zn(II) and Cd(II) in their complexes with a polytopic Mannich base ligand: a turn-on luminescence sensor for Zn(II) and detection of nitroaromatic explosives by the Zn(II) complexes

Avijit Das, Subrata Jana, and Ashutosh Ghosh

Cryst. Growth Des., **Just Accepted Manuscript** • DOI: 10.1021/acs.cgd.7b01752 • Publication Date (Web): 10 Mar 2018

Downloaded from http://pubs.acs.org on March 10, 2018

Just Accepted

"Just Accepted" manuscripts have been peer-reviewed and accepted for publication. They are posted online prior to technical editing, formatting for publication and author proofing. The American Chemical Society provides "Just Accepted" as a service to the research community to expedite the dissemination of scientific material as soon as possible after acceptance. "Just Accepted" manuscripts appear in full in PDF format accompanied by an HTML abstract. "Just Accepted" manuscripts have been fully peer reviewed, but should not be considered the official version of record. They are citable by the Digital Object Identifier (DOI®). "Just Accepted" is an optional service offered to authors. Therefore, the "Just Accepted" Web site may not include all articles that will be published in the journal. After a manuscript is technically edited and formatted, it will be removed from the "Just Accepted" Web site and published as an ASAP article. Note that technical editing may introduce minor changes to the manuscript text and/or graphics which could affect content, and all legal disclaimers and ethical guidelines that apply to the journal pertain. ACS cannot be held responsible for errors or consequences arising from the use of information contained in these "Just Accepted" manuscripts.

ACS Publications

is published by the American Chemical Society. 1155 Sixteenth Street N.W.,
Washington, DC 20036

Published by American Chemical Society. Copyright © American Chemical Society.
However, no copyright claim is made to original U.S. Government works, or works
produced by employees of any Commonwealth realm Crown government in the course
of their duties.

Modulation of nuclearity by Zn(II) and Cd(II) in their complexes with a polytopic Mannich base ligand: a turn-on luminescence sensor for Zn(II) and detection of nitroaromatic explosives by the Zn(II) complexes

Avijit Das, Subrata Jana, Ashutosh Ghosh*

Department of Chemistry, University College of Science, University of Calcutta, 92, A.P.C. Road, Kolkata 700009, India, E-mail address: ghosh_59@yahoo.com

Abstract

Reactions of Zn^{II} ion with the ligand H_2L (H_2L = N,N′-dimethyl-N,N′-bis(2-hydroxy-3-methoxy-5-methylbenzyl)ethylenediamine) in presence of bridging co-ligands, chloride, thiocyanate/acetate or azide/acetate yielded three new dinuclear complexes, $[Zn_2LCl_2(H_2O)]$ (**1**), $[Zn_2L(SCN)_2(H_2O)]\cdot H_2O$ (**2**), $[Zn_2L(N_3)(CH_3CO_2)]$ (**3**) whereas Cd^{II} ion formed three new tetranuclear complexes, $[Cd_4L_2Cl_4]\cdot H_2O$ (**4**), $[Cd_4L_2(SCN)_2(CH_3CO_2)_2]\cdot 2H_2O$ (**5**), $[Cd_4L_2(N_3)_2(CH_3CO_2)_2]\cdot 3H_2O$ (**6**) with the same ligand and co-ligands. The Zn^{II} ions are penta-coordinated in all of its complexes, **1-3** except one zinc centre in complex **3,** which is distorted tetrahedral. All four Cd^{II} centres in each of its complexes, **4** and **5** possess hexa-coordinated distorted octahedral geometry. In complex **6**, two Cd^{II} centers are hexa-coordinated and other two are hepta-coordinated. The deprotonated ligand (L^{2-}) is hexa-/hepta-dentate in the Zn^{II} complexes, **1-3** but octa-dentate in the Cd^{II} complexes, **4-6**. The differences in nuclearity and in the coordination modes of the ligands in the resulting complexes have been explained considering the preference for different coordination numbers of these two metal ions. H_2L exhibited highly specific, sensitive and selective turn-on fluorescence sensing property for Zn^{2+} ion. The mechanism of fluorescence enhancement, host guest binding stoichiometry and binding constant has also been calculated. The detection limit of Zn^{2+} ion is 7.69 nM, with binding constant $K=1.508 \times 10^{10}\ M^{-2}$. The produced Zn(II) complexes sense nitroaromatic explosives in solution *via* turn off florescence response. The solution phase sensing mechanism has been studied thoroughly. Remarkably, the limit of detection of picric acid is in ppt level (912, 910 and 896 ppt for complexes **1**, **2** and **3** respectively) having a strong quenching constant (K_{SV}) are 8.063×10^4 , 7.987×10^4 and $8.51 \times 10^4\ M^{-1}$ for complex **1**, **2** and **3** respectively.

Introduction

The rational design and synthesis of discrete multinuclear metal complexes have attracted substantial interest owing to their structural diversity, interesting magnetic properties and potential applications in the fields of catalysis, luminescence, gas adsorption and functional materials. [1-12] The structural variety and nuclearity of these types of complexes depend on various factors such as coordination number and geometry, charge of the metal ions, HSAB behavior of metal ion and donor atoms of the ligands, denticity, flexibility, shape and size of ligands and co-ligands etc.[13-15] There are some reports in literature where the polydentate Mannich base, N,N′-dimethyl-N,N′-bis(2-hydroxy-3-methoxy-5-methylbenzyl (H_2L) has been used as compartmental ligands to prepare some heterometallic M^{II}-Ln^{III}(M= Ni, Zn, Co and Ln = Tb, Dy, Gd) and homometallic Cu(II), Ni(II) complexes.[16-19] The complexes have been synthesized mainly with an aim to study their magnetic properties and it has been found that these complexes are either dinuclear or tetranuclear but there is no rationalization of factors on which the nuclearity of the complexes depends. Moreover, since the ligand is a good complexing agent due to its polytopic and chelating nature, it has the potential to be used as a sensor for various environmentally and biologically important metal ions, which is still remained unexplored.

Recently, several groups are engaged in the specific design and synthesis of chemical sensors for the specific detection of metal ions, anions, various poisonous organic analytes and explosives because of their significant influences on environment and human life.[20-29] Among various metal ions, Zn^{2+} is second most important metal ion in mammalian body after iron.[30,31] On the other hand, Cd^{2+} is known as an extremely toxic and potentially carcinogenic metal.[32] These two metal ions are also having some potential applications in the field of material chemistry as light-emitting diodes, luminescent probes, photovoltaic devices and photocatalyst for the degradation of organic dyes.[33-39] A lot of fluorescence chemosensors for Zn^{2+} and Cd^{2+} ions have been reported in literature; among them, turn-on fluorescent sensors have great advantages in molecular recognition and as sensing materials.[40-42] However, most of such sensors cannot distinguish metal ions like Zn^{2+}, Cd^{2+} and Hg^{2+} which exhibit similar spectral and chemical properties due to d^{10} electronic configuration and show chelation enhanced fluorescence (CHEF)[43,44] and photoinduced electron transfer (PET)[45,46] effects of the ligands upon coordination. Thus, it is a great challenge to design a highly specific and selective turn-on fluorescent sensor for Zn^{2+}.

Among various organic analytes, nitroaromatic compounds are of special concern because they are serious pollution sources of environment and other security applications due to their explosivity and high toxicity.[47,48] So, the rapid and highly effective detection of nitroaromatic explosives is an important area of current research due to homeland security, environmental and public safety.[49] Various methods of explosives detection with high selectivity are currently available like metal detectors, gas chromatography, trained surface enhanced Raman spectroscopy, cyclic voltammetry etc.[50,51] but they are usually expensive, inconvenient and not very easy to handle. On the other hand, fluorescence based detection have recently been considered as one of the most promising techniques for explosive detection due to their cost effectiveness, ease of operation, high selectivity, portability, and the ability to be applied in both solution and solid phases.[52-54]

Herein, we have synthesized and structurally characterized six discrete polynuclear Zn(II) and Cd(II) complexes, $[Zn_2LCl_2(H_2O)]$ (**1**), $[Zn_2L(SCN)_2(H_2O)]\cdot H_2O$ (**2**), $[Zn_2L(N_3)(CH_3CO_2)]$ (**3**) $[Cd_4L_2Cl_4]\cdot H_2O$ (**4**), $[Cd_4L_2(SCN)_2(CH_3CO_2)_2]\cdot 2H_2O$ (**5**), $[Cd_4L_2(N_3)_2(CH_3CO_2)_2]\cdot 3H_2O$ (**6**) using the ligand H_2L to investigate the influence of metal ion in controlling the nuclearity of the complexes. All three complexes of Zn(II) are dinuclear and those three of Cd(II) are tetranuclear. This difference is explained considering the preferences for the coordination numbers and geometries of these two metal ions. The sensing behavior of the ligand, H_2L is explored for the first time in this work. The ligand acts as turn-on fluorescence chemosensor for the selective detection Zn^{2+} ion. Again the Zn(II) complexes **1-3** have been found to act as turn-off fluorescence chemosensor for highly selective detection of nitroaromatic explosives in the ppt level.

Experimental Section

All chemicals were of reagent grade and were commercially available. They were used without further purification.

Synthesis of ligand H_2L

The Mannich base ligand H_2L was synthesized by a following standard literature method.[16-19] Briefly, 5 mmol of N,N′-dimethylethylenediamine (0.55 mL) was stirred with 10 mmol of formaldehyde (0.3 mL) for 1hr in methanol solvent (25 mL). After the addition of 10 mmol

2-methoxy-4-methylphenol (1.26 ml), the resulting solution was refluxed for about 5 hr. and allowed to cool for one day. Then the appeared white colored ligand was washed with methanol and collected for experiment.

Yield 1.164 g (60%). $C_{22}H_{32}N_2O_4$ (388.5). Calculated C, 68.01; H, 8.30; N, 7.21; Found C, 68.05; H, 8.20; N, 7.30; ESI-MS (positive ion mode, CH_3OH) calculated. m/z 388.24, found 389.31 (100%, $[H_2L+1]^+$). ^{1}H NMR (300 MHz, DMSO-d^6, ppm): δ 6.63 (s, 2H), δ 6.49 (s, 2H), δ 3.69 (s, 6H), δ 3.53 (s, 6H), δ 2.53 (s, 4H), δ 2.14 (s, 6H), δ 2.12 (s, 6H) 1.22. UV/Vis: λ_{max} = 285 nm. IR: $\nu_{(O–H)}$ = 3436 cm^{-1}, $\nu_{(C–O)}$ =1239 cm^{-1}.

*Synthesis of the complex [Zn$_2$LCl$_2$(H$_2$O)] (**1**)*

A methanol solution (10 ml) of zinc chloride (2 mmol, 272 mg) was added to the methanol solution (20 ml) of ligand H_2L (1 mmol, 388 mg) with stirring. The resulting solution was stirred further for ca. 1 h. Diffraction quality single crystals were obtained after a few days on slow diffusion of diethyl ether into the mother liquor.

Yield 0.212 g (70%). $C_{22}H_{32}Cl_2N_2O_5Zn_2$ (606.18). Calculated C, 43.59; H, 5.32; N, 4.62; Found C, 43.50; H, 5.50; N, 4.70; ESI-MS (positive ion mode, CH_3OH) calculated. m/z 604.02, found 605.09 (100%, $[Zn_2LCl_2(H_2O)+1]^+$). ^{1}H NMR (300 MHz, DMSO-d^6, ppm): δ 6.59 (s, 2H), δ 6.36 (s, 2H), δ 3.65 (s, 6H), δ 3.38 (s, 6H), δ 2.11 (s, 6H), δ 2.10 (s, 6H). UV/Vis: λ_{max} = 242 and 291 nm. IR: $\nu_{(O–H)}$ = 3431 cm^{-1}, $\nu_{(C–O)}$ =1253 cm^{-1}.

*Synthesis of the complex [Zn$_2$L(SCN)$_2$(H$_2$O)]·H$_2$O (**2**)*

A solution of zinc acetate dihydrate (2 mmol, 439 mg) in 10 mL methanol, was added to a methanolic solution (20 mL) of ligand H_2L (1 mmol, 388 mg) with stirring. Then a 1:1 methanol/water solution of sodium thiocyanate (2 mmol, 162 mg) was added to the mixture. The resulting solution was stirred further for ca. 2 h. Single crystals suitable for X-ray diffraction were obtained by slow evaporation of methanol solution in open atmosphere after few days.

Yield 0.230 g (69%) $C_{24}H_{32}N_4O_6S_2Zn_2$ (667.44). Calculated C, 43.19; H, 4.83; N, 8.39; Found C, 43.30; H, 4.70; N, 8.50; ESI-MS (positive ion mode, CH_3OH) calculated. m/z 574.05, found 574.05 (100%, $[Zn_2(L)SCN]^+$). ^{1}H NMR (300 MHz, DMSO-d^6, ppm): δ 6.72 (s, 2H), δ 6.47 (s, 2H), δ 3.79 (s, 6H), δ 3.50 (s, 6H), δ 2.22 (s, 6H), δ 2.19 (s, 6H). UV/Vis: λ_{max} = 239 and 291 nm. IR: $\nu_{(O–H)}$ = 3418 cm^{-1}, $\nu_{(SCN)}$ = 2084 cm^{-1}, $\nu_{(C–O)}$ =1254 cm^{-1}.

*Synthesis of the complex [$Zn_2L(N_3)(CH_3CO_2)$] (**3**)*

Complex **3** was synthesized in a similar method to that of complex **2** except that sodium azide (2 mmol, 130 mg) was used instead of sodium thiocyanate. Colourless single crystals were obtained after few days by the slow evaporation of methanol solution.

Yield 0.235 g (76%). $C_{24}H_{33}N_5O_6Zn_2$ (618.33). Calculated C, 46.62; H, 5.38; N, 11.33; Found C, 46.70; H, 5.50; N, 11.20; ESI-MS (positive ion mode, CH_3OH) calculated. m/z 575.11, found 575.09 (100%, $[Zn_2(L)N_3]^+$). ^1H NMR (300 MHz, DMSO-d^6, ppm): δ 6.57 (s, 2H), δ 6.35 (s, 2H), δ 3.64 (s, 6H), δ 3.38 (s, 6H), δ 2.08 (s, 6H), δ 1.68 (s, 3H). UV/Vis: λ_{max} = 242 and 293 nm. IR: $\nu_{(O–H)} = 3410$ cm^{-1},$\nu_{(N3)} = 2077$ cm^{-1}, $\nu_{(C–O)} = 1253$ cm^{-1}.

*Synthesis of the complex [$Cd_4L_2Cl_4$]·H_2O (**4**)*

A 1:1 water methanol solution (10 ml) of cadmium chloride (2 mmol, 272 mg) was added to the methanol solution (20 ml) of ligand H_2L (1 mmol, 388 mg) with stirring. The resulting solution was stirred further for ca. 1 h. Diffraction quality single crystals were obtained after a few days on slow diffusion of diethyl ether into the mother liquor.

Yield 0.260 g (75%). $C_{44}H_{62}Cd_4Cl_4N_4O_9$ (1382.44). Calculated C, 38.23; H, 4.52; N, 4.05; Found C, 38.30; H, 4.60; N, 4.10; UV/Vis: λ_{max} = 244 and 298 nm. IR: $\nu_{(O–H)} = 3431$ cm^{-1}, $\nu_{(C–O)} = 1250$ cm^{-1}.

*Synthesis of the complex [$Cd_4L_2(SCN)_2(CH_3CO_2)_2$]·$2H_2O$ (**5**)*

A solution of cadmium acetate dihydrate (2 mmol, 533 mg) in 10 mL methanol, was added to a methanolic solution (20 mL) of ligand H_2L (1 mmol, 388 mg) with stirring. Then a 1:1 methanol/water solution of sodium thiocyanate (2 mmol, 162 mg) was added to the mixture. The resulting solution was stirred further for ca. 2 h. Single crystals suitable for X-ray diffraction were obtained by slow evaporation of methanol solution in open atmosphere after few days.

Yield 0.268 g (72%) $C_{50}H_{66}Cd_4N_6O_{14}S_2$ (1488.86). Calculated C, 40.34; H, 4.47; N, 5.64; Found C, 40.40; H, 4.30; N, 5.80; UV/Vis: λ_{max} = 264 and 290 nm. IR: $\nu_{(O–H)} = 3408$ cm^{-1} , $\nu_{(SCN)} = 2077$ cm^{-1}, $\nu_{(C–O)} = 1247$ cm^{-1}.

*Synthesis of the complex [$Cd_4L_2(N_3)_2(CH_3CO_2)_2$]·$3H_2O$ (**6**)*

Complex **6** was synthesized in a similar method to that of complex **5** except that sodium azide (2 mmol, 130 mg) was used instead of sodium thiocyanate. Colourless single crystals were obtained after few days by the slow evaporation of methanol solution.

Yield 0.262 g (71%). $C_{48}H_{68}Cd_4N_{10}O_{15}$ (1474.76). Calculated C, 39.09; H, 4.65; N, 9.50; Found C, 39.20; H, 4.50; N, 9.60; UV/Vis: λ_{max} = 252 and 294nm. IR: $\nu_{(O–H)}$ = 3430 cm^{-1}, $\nu_{(N3)}$ = 2066 cm^{-1}, $\nu_{(C–O)}$ =1255 cm^{-1}.

Physical measurements

Elemental analyses (C, H and N) were performed using a Perkin–Elmer 2400 series II CHN analyzer. IR spectra in KBr pellets (4000–500 cm^{-1}) were recorded using a Perkin-Elmer RXI FT-IR spectrophotometer. The electronic absorption spectra (800–200 nm) in methanol solution were collected in a Hitachi U-3501 spectrophotometer. The steady-state fluorescence emission spectra were recorded using a PerkinElmer LS-55 spectrofluorimeter after proper background correction with individual solvents in quartz cells with 1 cm path length. The decay times of the zinc complexes **1-3** and ligand in the micro seconds region were also acquired by fluorescence decay mode in QM-30 fluorimeter from PTI, U.S.A. The decay parameters were recovered using a nonlinear iterative fitting procedure based on the Marquardt algorithm. ^{1}HNMR spectra were recorded in DMSO-d_6 on a 300 MHz instrument (Bruker), where tetramethylsilane (TMS) was used as an internal standard. ESI mass spectra were recorded on a WATERS Xevo G2-S QTof mass spectrometer in HRMS grade methanol. The fluorescence quantum yield (Φ_F) of ligand and zinc complexes **1-3** were calculated using tryptophan as reference standard in water having quantum yield (Φ_R) 0.13, following the equation

$$\frac{\Phi_S}{\Phi_R} = \frac{A_S}{A_R} \times \frac{(Abs)_R}{(Abs)_S} \times \frac{\eta_S^2}{\eta_R^2}$$

Where the subscripts S and R stands for sample and reference standard respectively, Φ is the fluorescence quantum yield, A is integrated area under fluorescence curve, Abs is absorbance; η is the refractive index of the solvent.[45]

X-ray Crystallographic data collection and refinement

Suitable single crystals of complexes **1-6** were mounted on a Bruker-AXS SMART APEXII diffractometer equipped with a graphite monochromator and Mo-Kα (λ = 0.71073Å) radiation. The structure was solved by direct methods and refined by full-matrix least squares on F^2 using the SHELXL-2014 package.[55] Non-hydrogen atoms were refined with anisotropic thermal parameters. Hydrogen atoms attached with oxygen atoms of water molecules in complexes **1** and **2** were located by difference Fourier maps and were kept at fixed positions. All other hydrogen atoms were placed in their geometrically idealized positions and constrained to ride on their parent atoms. Successful convergence was indicated by the maximum shift/error of 0.001 for the last cycle of the least squares refinement. Absorption corrections were carried out using the SADABS program.[56] Data collection, structure refinement parameters and crystallographic data for complexes **1-6** are given in Table 1.

Results and discussion

Syntheses of the complexes

The ligand H_2L was prepared by the Mannich reaction between 2-methoxy-4-methylphenol, N,N′-dimethylethylenediamine and formaldehyde following literature method and characterized by Mass and NMR spectroscopy (figures S1 and S2, Supporting Information).[16-19] The reaction of various zinc salts (zinc chloride/zinc acetate) with the ligand H_2L in 1:2 ratios in presence of chloride or pseudohalides (azide/thiocyanate) produces complexes **1-3**. The ligand acts as a compartmental hexa-/heptadentate (N_2O_4) ligand and coordinated to two metal centres (Scheme 1).The penta-coordination geometry of the Zn(II) is completed by the solvent molecules and/or anionic coligands. All zinc complexes are characterized by elemental analysis, IR, UV-Vis, Mass (figures S3-S5, Supporting Information) and ^{1}H NMR (figure S6-S8, Supporting Information) spectroscopy. The cadmium complexes **4-6** have been prepared following the similar methods by reacting ligand H_2L with cadmium salts in 1:2 ratios in presence of azide or thiocyanate or acetate or chloride co-ligands. All three Cd(II) complexes possess tetranuclear structures where Cd(II) centers are either six-coordinated or seven-coordinated. The structure of all complexes are confirmed by single crystal X-ray diffraction.

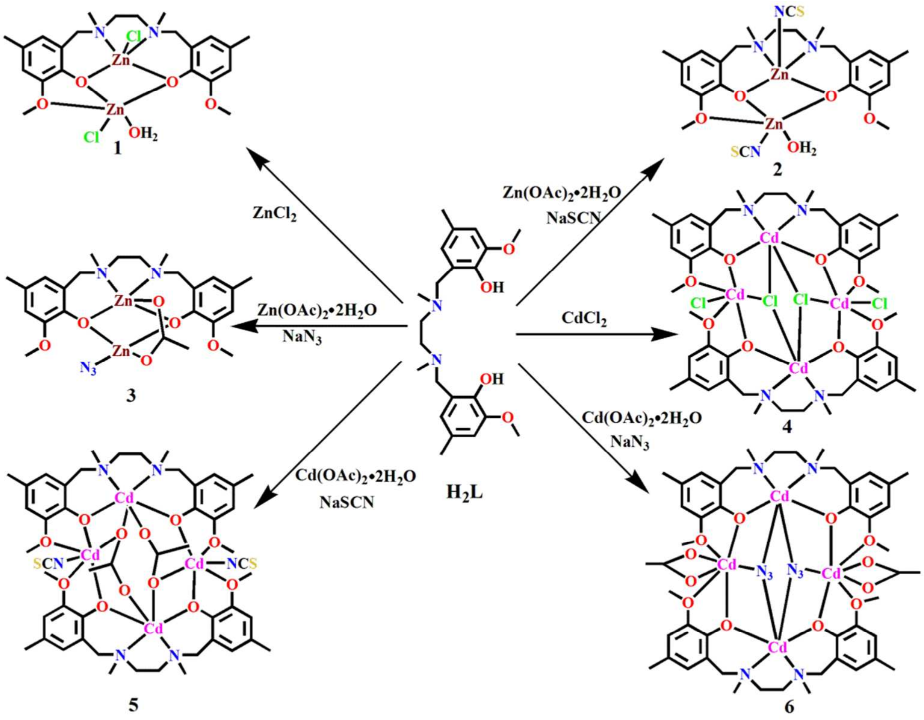

Scheme 1: Synthesis of complexes **1-6**

IR and UV–Vis spectra of Complexes

In the IR spectra of complexes **1** and **2**, bands around 3400 cm^{-1} are observed due to the presence of the coordinated water molecule. A strong absorption bands appear around 2080 cm^{-1} in the IR spectra of complexes **2** and **5**, indicating the presence of thiocyanate groups.[57] In the IR spectra of complexes **3** and **6,** strong bands around 2070 cm^{-1} are observed which indicates the presence of terminal azide groups.[58] The electronic spectra of all complexes are recorded in methanol. All complexes show absorption bands in the UV region due to charge transfer transitions.

Description of the structures

*Complexes **1-3***

Single crystal X-ray diffraction studies reveal that all three zinc complexes **1-3** have dinuclear structure where both zinc centers have penta-coordinated geometry except complex **3** where one zinc centre is distorted tetrahedral. The Addison parameter[59] (trigonality index, $\tau = (\alpha - \beta)/60$, where α and β are the two largest L-M-L angles of the coordination sphere) for Zn1 are 0.423, 0.496 and 0.151 in complexes **1, 2** and **3**, respectively and this confirms that the geometry is intermediate between square pyramid and trigonal bipyramid ($\tau = 0$ for a perfect square pyramid and a $\tau = 1$ for a perfect trigonal bipyramid) for complex **2,** highly distorted square pyramid for **1** and slightly distorted square pyramid for **3.** The Addison parameters (τ) for Zn2 are 0.259 and 0.381 in complexes **1** and **2** respectively confirming the distorted square pyramidal character. The asymmetric units of complexes **1-3** with selective atom numbering scheme are shown in figures 1, 2 and 3, respectively. Penta-coordinated Zn1 centre is equatorially coordinated by two nitrogen atoms (N1 and N2) and two oxygen atoms (O1 and O2) of the deprotonated Mannich base ligand L^{2-}. The fifth coordination site is occupied by chloride ion Cl1 for **1**, nitrogen atom N3 from thiocyanate ion for **2**, oxygen atom O6 from acetate ion for **3**. In complexes **1** and **2**, Zn2 centre is equatorially cordinated by four oxygen atoms (O1, O2 and O3 from ligand L^{2-}, O5 from water molecule) and axially by chloride ion Cl2 for **1**, nitrogen atom N4 from thiocyanate ion for **2**. In complex **3**, Zn2 center is tetrahedrally coordinated by three oxygen atoms (O1 and O2 from ligand L^{2-}, O5 from acetate ion) and one nitrogen atom N3 from azide ion. Zn-N bond distances are within the range of 1.90-2.23Å. Zn-O bond distances are within the range of 1.97-2.47Å. Selected bond lengths and bond angles of all three complexes are given in Table S1(Supporting Information). The intramolecular Zn-Zn distances are 3.125(4)Å, 3.078(1)Å and 2.903(6)Å in complexes **1**, **2** and **3** respectively.

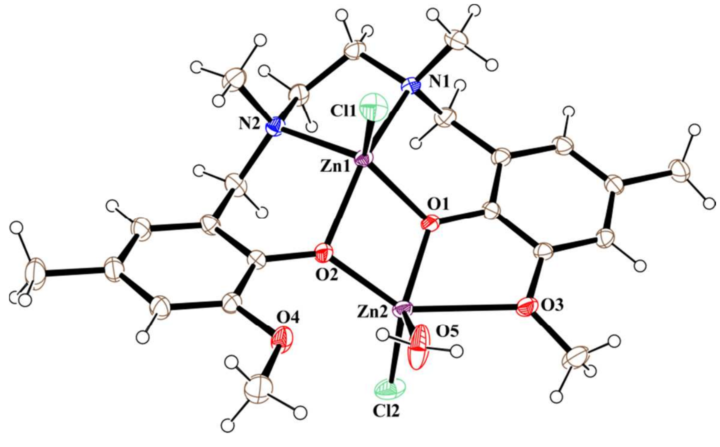

Figure 1: ORTEP view of complex **1** with 30% ellipsoid probability.

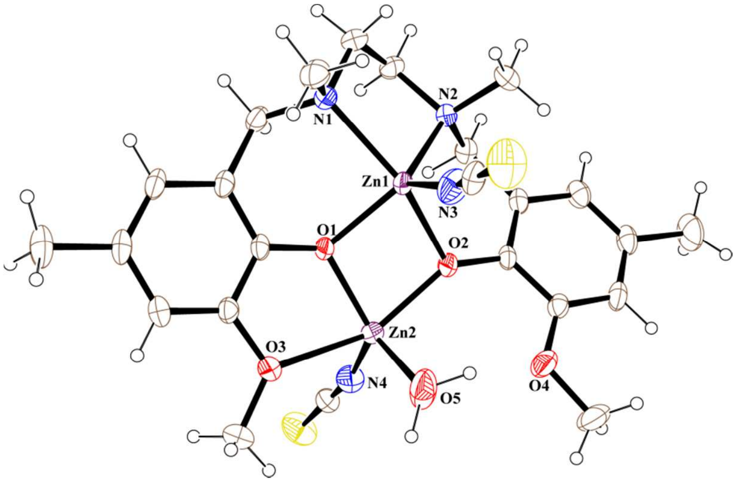

Figure 2: ORTEP view of complex **2** with 30% ellipsoid probability. Solvent water molecule is not shown for clarity.

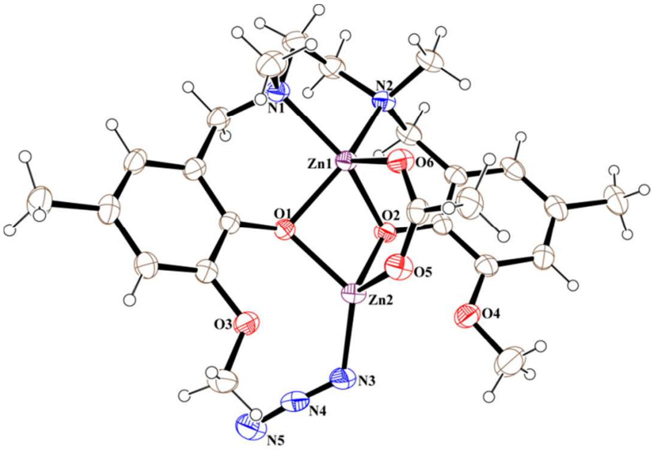

Figure 3: ORTEP view of complex **3** with 30% ellipsoid probability.

In complex **1**, the hydrogen atom, H(2w), attached with O(5) of the coordinated water molecule is engaged in intermolecular hydrogen bond formation with the symmetry related chlorine atom,Cl2$^{\#}$ ($^{\#}$= x, 1.5-y,0.5+z) of the other molecule to form a helical chain (figure 4). The hydrogen atom, H(1w), attached with O(5) of the coordinated water molecule is also engaged in intra-molecular hydrogen bond with the methoxy oxygen atom O4. Similarly, in complex **2**, The hydrogen atom, H(2w), attached with O(5) of the coordinated water molecule is engaged in intermolecular hydrogen bond formation with the symmetry related oxygen atom, O6$^{\$}$ ($^{\$}$= x, -1+y, z) of the water molecule (figure 5). The hydrogen atom, H(1w), attached with O(5) of the coordinated water molecule is also engaged in intramolecular hydrogen bond with the methoxy oxygen atom O4. Details geometrical features of these hydrogen bonding interactions are given in Table S2 (Supporting Information).

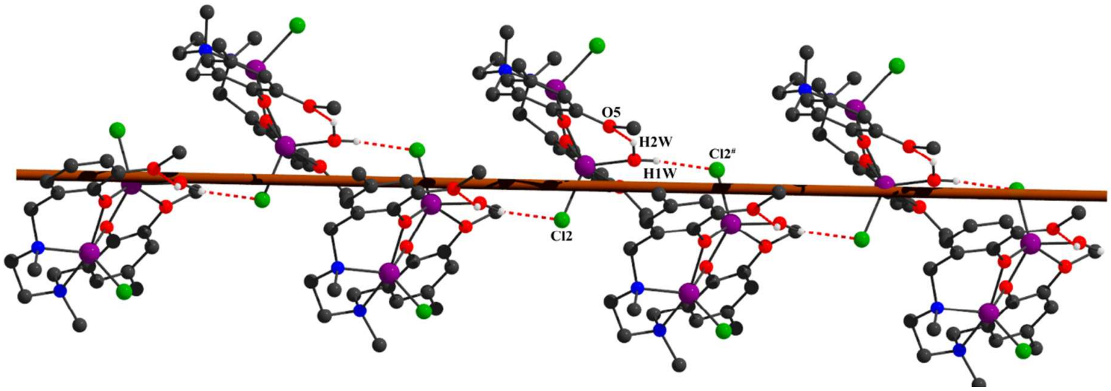

Figure 4: Hydrogen bonded helical chain of complex **1**. All hydrogen atoms except water molecules are omitted for clarity. $^{\#}$= x, 1.5-y,0.5+z.

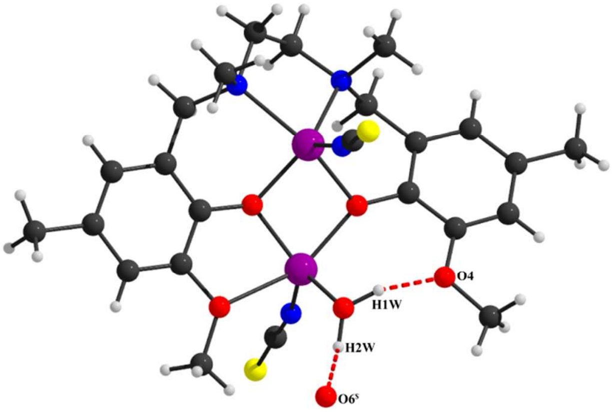

Figure 5: Hydrogen bonding interactions in complex **2**. $^{\$}$= x, -1+y, z.

*Complexes **4-6***

All three complexes possess very similar tetranuclear structures with double open cubane core where all four Cd(II) centres have hexa-coordinated distorted octahedral geometry except complex **6** where two Cd(II) centers are hepta-coordinated distorted pentagonal bipyramid. The asymmetric unit of all complexes contain four Cd(II) ions except complex **6** where two centrosymmetric independent units are present with two Cd(II) ions in each unit, two deprotonated Mannich base ligands L^{2-} and four co-anions (chloride in **4**, acetate and thiocyanate in **5,** acetate and azide in **6**). The coordination environments of Cd1 and Cd3 are almost similar to that of Cd2 and Cd4 respectively, only very small difference in bond distances and angles in complexes **4** and **5**, but for complex **6**, these are identical due to the presence of a centre of symmetry (1-x, -y, -z). Selected bond lengths and bond angles of all three complexes are given in Table S3(Supporting Information).

Complex **4** is a double μ_3 chloride bridged tetranuclear complex where four Cd(II) centres are bridged by two chloride ions. Cd1 and Cd2 centres are coordinated by four ONNO donor atoms respectively from each of the two ligands H_2L (O1, N1, N2, O2 for Cd1 and O5, N3, N4, O6 for Cd2) and two μ_3 bridged chloride ions Cl1 and Cl2. Cd3 and Cd4 centres are coordinated by four oxygen atoms from two H_2L ligands and one μ_3 bridged and one terminal chloride ions. Perspective view of the asymmetric unit of complex **4** is shown in figure 6 with selective atom numbering scheme.

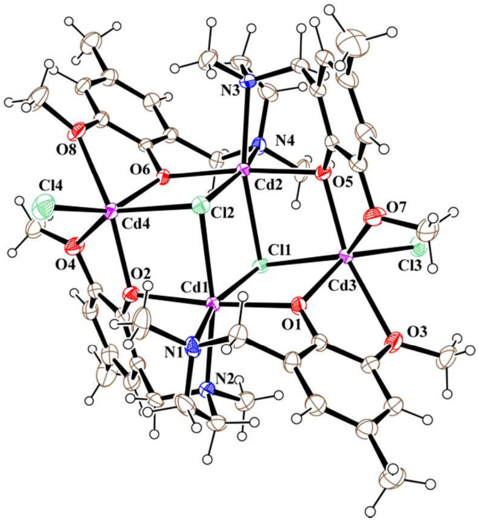

Figure 6: ORTEP view of complex **4** with 30% ellipsoid probability. Solvent water molecule is not shown for clarity.

In complex **5**, two Cd(II) centers Cd1 and Cd2 are coordinated by four ONNO atoms of the specific Mannich base ligand H_2L (O1, N1, N2, O2 for Cd1 and O5, N3, N4, O6 for Cd2) and two oxygen atoms of μ_3 bridging acetate ions (O9, O10 for Cd1and O11, O12 for Cd2). Cd3 and Cd4 centres are also hexa-coordinated being bonded to four oxygen atoms of two ligands H_2L (O1, O3 O5 and O7 for Cd3 and O2, O4, O6 and O8 for Cd4) and another two sites are coordinated by one oxygen atom (O11 for Cd3 and O12 for Cd4) of bridging acetate group and one nitrogen atom (N5 for Cd3 and N6 for Cd4) of terminal thiocyanate group. In this complex, acetate bridges among three Cd(II) centers via tridentate (μ_3-$1\kappa O:2\kappa^2 O,O'$) bridging mode where one oxygen atom bridges two Cd(II) centres in a μ_2-

fashion and other oxygen atom coordinates to another Cd(II) center. So, all four Cd(II) centres are interconnected through two acetate groups. ORTEP view of the asymmetric unit of complex **5** is shown in figure 7 with selective atom numbering scheme.

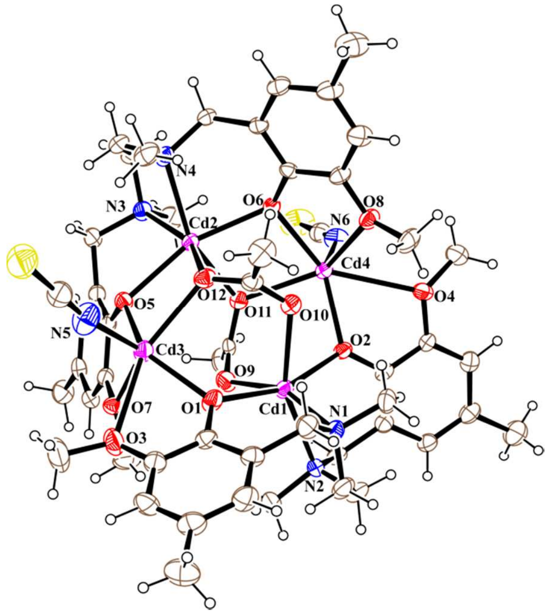

Figure 7: ORTEP view of complex **5** with 30% ellipsoid probability. Solvent water molecules are not shown for clarity.

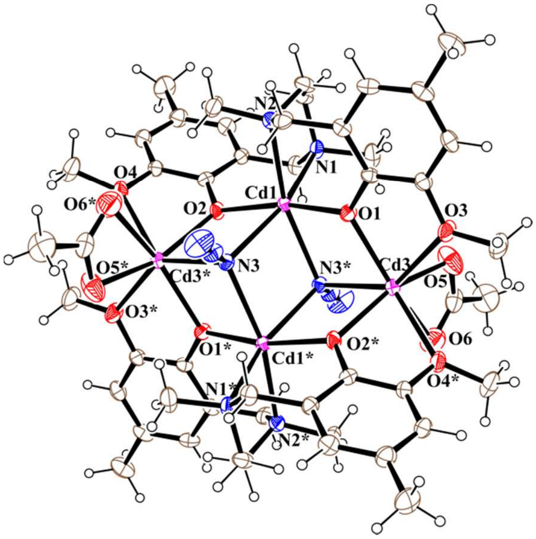

Figure 8: ORTEP view of complex **6A** with 30% ellipsoid probability. Solvent water molecules are not shown for clarity. *= 1-x, -y, -z.

The structure of complex **6** contains two independent units (called A and B) both with crystallographic centers of symmetry. Both units have identical structures with slight differences in bond angles and bond distances. A perspective view of molecules A and B are shown together with the atom numbering scheme respectively in figures 8 and S9 (Supporting Information). Cd1 centre is hexa-coordinated being bonded to four donor atoms O1, N1, N2 and O2 from the ligand H_2L and two symmetry related μ_3 bridging nitrogen atoms N3 and N3*(*= 1-x, -y, -z) from two azide. Cd3 centre is hepta-coordinated by four oxygen atoms O1, O3, O2*, O4*(*= 1-x, -y, -z) of two symmetry related ligands and μ_3 bridging nitrogen atoms N3* from azide and two oxygen atoms O5 and O6 from acetate ion in bidentate fashion.

It is worthy to note that herein, we have used same polydentate Manich base ligand H_2L, co-ligands (chloride, azide, thiocyanate and acetate) and reaction conditions for the syntheses of the Zn(II) and Cd(II) complexes but we got dinuclear complexes for Zn(II) and tetranuclear complexes for Cd(II). The size and coordination number of Cd(II) are greater than those of Zn(II). Zn(II) usually prefers four-coordinated or five-coordinated geometry whereas Cd(II) prefers coordination number six or higher. In all three Zn(II) complexes **1**-**3**, the deprotonated Manich base ligand L^{2-} acts as hexa-/hepta-dentate ligand and binds two Zn(II) centres; the anions (azide, thiocyanate, chloride) are cordinated as terminal ligands except acetate ion which bridges two Zn(II) centres in μ_2-1κO:2κO fashion. On the other hand, for Cd(II) complexes **4-6**, each deprtonated Mannich base ligand L^{2-} acts as an octa-dentate ligand to fulfil higher coordination number of Cd(II) and coordinates simultaneously to three Cd(II) centres. Moreover, in all three complexes two of the anionic co-ligands (azide, acetate, chloride) also bridge three Cd(II) centres in μ_3-fashion to satisfy its coordination number and to hold the four Cd(II) centres together. For Cd(II) complexes, the μ_3-bridging modes of acetate and chloride ions are well known but it is rare in case azide ion; only four μ_3-azide bridged Cd(II) complexes are reported in literature till date.[60-63]

Luminescent Properties

The ligand H_2L and Zn(II) complexes **1-3** show fluorescence upon excitation at 290 nm in methanol solution and the emission occurs in the range of 300-450 nm (figure 9). The emission maxima for ligand H_2L, occurs at 327 nm whereas the emission maxima for Zn(II) complexes **1-3** appear at 347 nm. From the spectra it is clear that fluorescence intensity of zinc complexes (**1-3**) are about 10-fold higher compared to ligand H_2L and the emission maximum is red shifted around 20 nm may be due to the strong electronic coupling between the neighbouring ligands through Zn(II) ions.

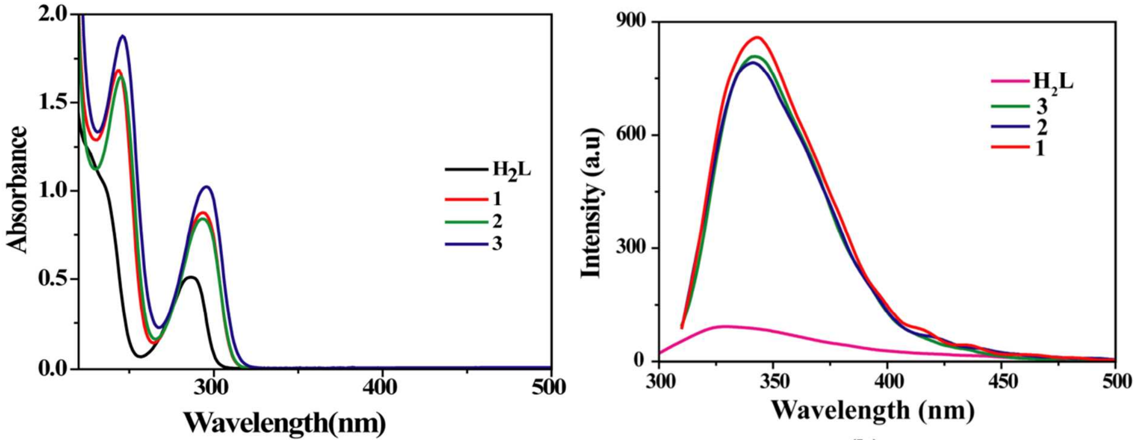

(a) (b)

Figure 9: (a) UV-VIS and (b) Fluorescence spectra of ligand and complexes **1-3** in methanol (excitation wavelength 290 nm and conc. 10^{-4} M).

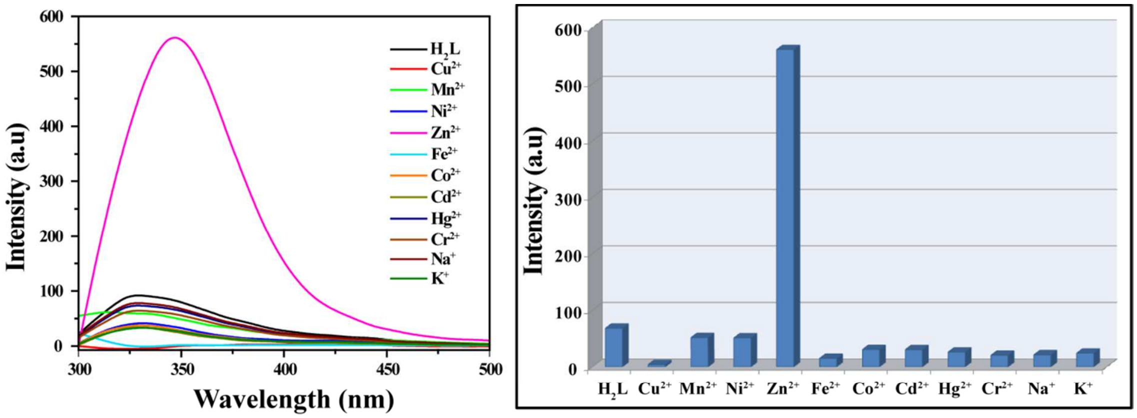

(a) (b)

Figure 10: (a) Fluorescence spectra of ligand H_2L (excitation wavelength 290 nm and conc. 10^{-5} M) in presence of various metal ions (2.0 equivalent) (b) Relative fluorescence intensity of ligand H_2L in presence of various metal ions.

In order to evaluate the sensing behaviour of ligand H_2L, the fluorescence spectra of H_2L is measured in presence of various metal ions e.g. Cr^{2+}, Mn^{2+}, Fe^{2+}, Co^{2+}, Ni^{2+}, Cu^{2+}, Cd^{2+}, Hg^{2+}, Na^{+}, K^{+} and Zn^{2+}. However, except for Zn^{2+} ion (where about 10-fold enhancement in fluorescence intensity occurs) no significant change in fluorescence intensity is observed on addition of the metal ions as shown in figure 10. This result indicates that ligand H_2L acts as a highly selective fluorescence only for Zn^{2+} ion. The florescence quantum yields for H_2L and complexes **1-3** are 0.013,0.055,0.052 and 0.054, respectively.

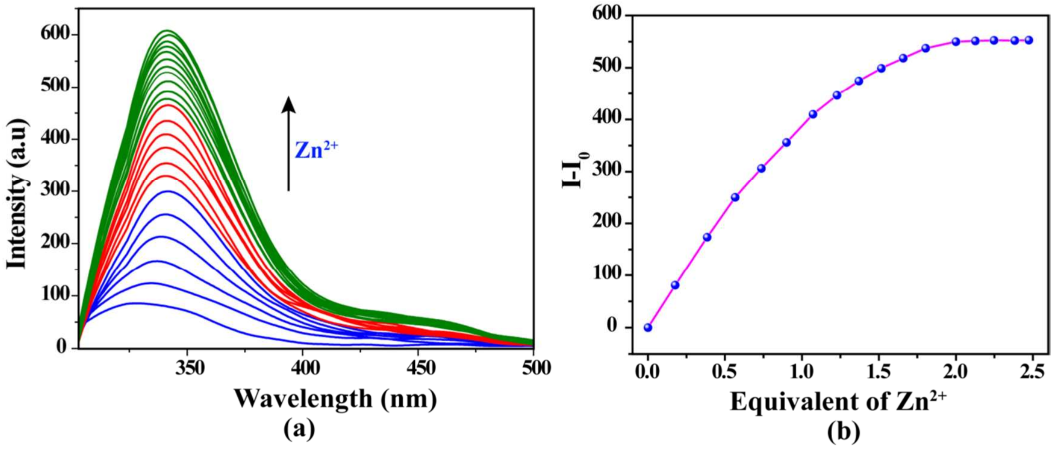

Figure 11: (a) Fluorescence titration of ligand H_2L with Zn^{2+} ion in methanol at room temperature (excitation wavelength 290 nm and conc. 10^{-5} M). (b) change in fluorescence intensity with the equivalent of Zn^{2+} ion added.

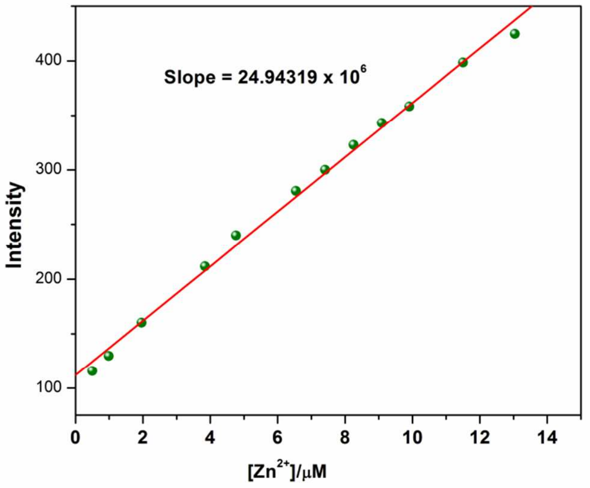

Figure 12: Determination of detection limit of ligand H_2L towards Zn^{2+} ion.

The fluorescence titration of ligand H_2L in methanol is carried out by the gradual addition of Zn^{2+} ion (using $ZnCl_2$) (figure 11). The fluorescence intensity increases linearly, indicating that Zn^{2+} is quantitatively bound to ligand H_2L and shows excellent sensitivity with a detection limit of 7.69 nM, which is better than most of the reported fluorescence sensors for zinc ion.[64-66] The detection limit is calculated using standard literature method (Equation 1, Supporting information) is shown in figure 12. [65]

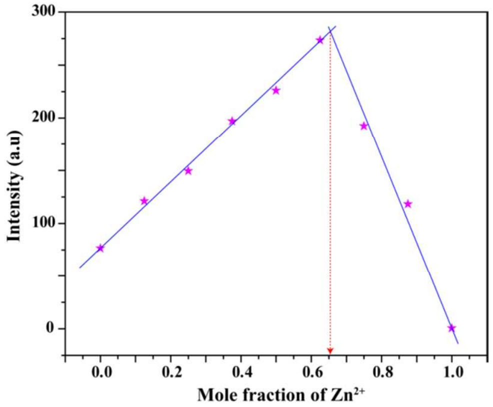

Figure 13: Job's plot for determining the stoichiometry of H_2L and Zn^{2+} ion.

The binding stoichiometry of ligand with Zn^{2+} is calculated from the Job's plot (figure 13). Job's plot is derived using fluorescence titration experiment and maximum fluorescence intensity is observed when the mole fraction of the Zn^{2+} ions is about 0.66, which implied a 1:2 ratio (H_2L:Zn^{2+}) complex formation which is also confirmed from single crystal X-ray structure. The binding constant K is 1.508×10^{10} M^{-2} obtained from the Benesi-Hilderbrand (Equation 2, Supporting information) plot as seen in figure 14.[67] Alternatively, the binding constant, K for binding Zn(II) with ligand H_2L in 1:2 ratio (H_2L:Zn^{2+}) is also calculated using the fluorescence titration data using a reported method (Equation 3, Supporting information) other than the Benesi-Hilderbrand method.[68-70] The binding constant K is 1.624×10^{10} M^{-2} calculated from figure S10 (Supporting information). Values obtained for K from two different methods of calculations corroborate each other.

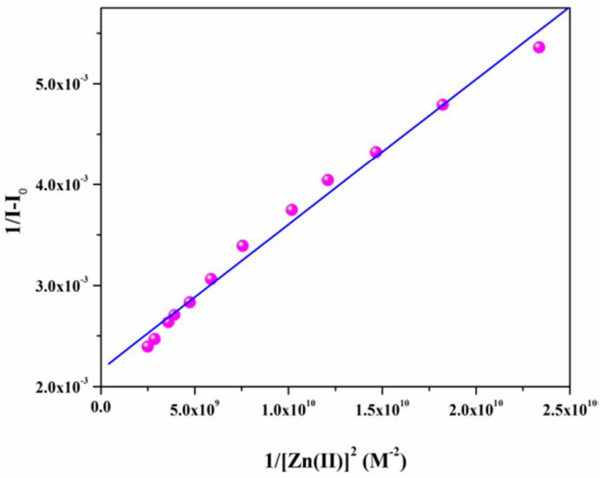

Figure 14: Benesi-Hilderbrand plot for H_2L and Zn(II) complex formation.

The fluorescence lifetimes of ligand H_2L and complexes **1-3** are measured in methanol solution at room temperature (figure 15). Decay profiles are fitted to a multi-exponential model (Equation 4, Supporting information) and average life time (τ_{av}) is calculated using following literature methods (Equation 5, Supporting information).[71] The average life times are given in Table 2. The average lifetime values of ligand H_2L decreases upon complex formation with Zn(II). In the free ligand (H_2L), intramolecular hydrogen bonding interactions between the hydrogen atoms of phenolic-OH groups and the amine nitrogen atoms impose some rigidity in the structure and restricted the nonradiative decays via rotational and vibrational relaxation pathways. This rigidification further increases due to complex formation with Zn(II). As a consequence, the fluorescence emission maxima and intensity of the ligand H_2L increases upon complex formation with Zn(II) and resulting in an increase in radiative decay rate of Zn(II) complex as compared to that of H_2L and lifetime values decreases.[72]

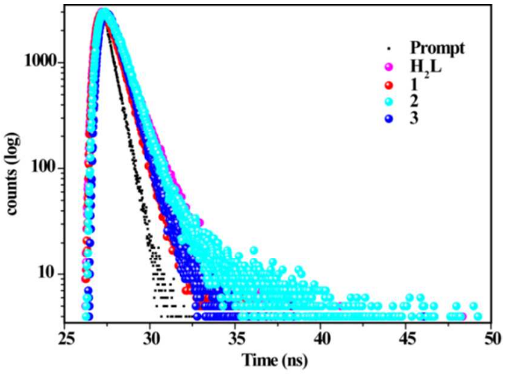

Figure 15: Fluorescence decay profile of ligand and complexes **1-3** in methanol.

The enhancement of fluorescence intensity of Zn(II) complexes **1**-**3** compared to the Mannich base ligand H_2L may be due to chelation enhancement of fluorescence emission (CHEF).[43,44] In the free ligand the lone pair of electrons present in two nitrogen atoms quench the fluorescence of the ligand H_2L due to photo induced electron transfer (PET).[45,46] On complex formation, the binding of ligand to the metal ions causes an increase in rigidity in structure and block the PET process and fluorescence intensity increases.

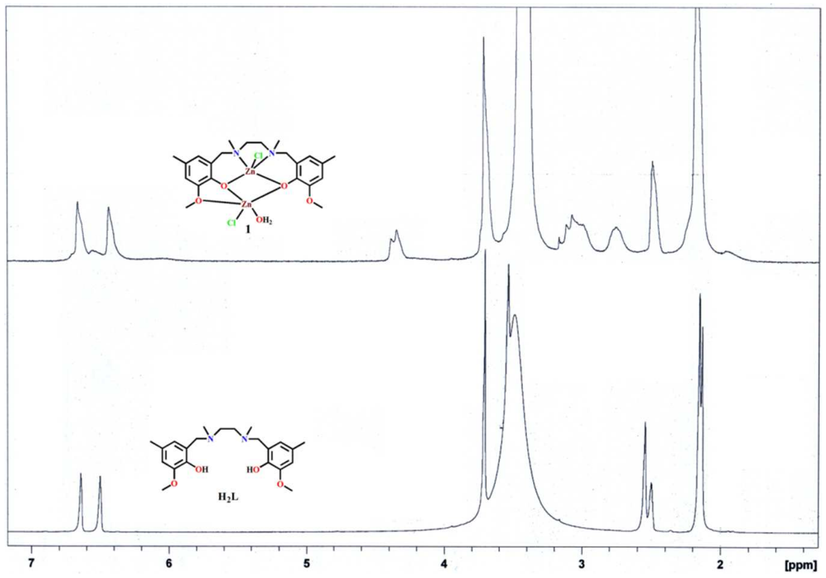

Figure 16: ^{1}H NMR spectra of ligand and complex **1** in DMSO-d$_6$.

The ^{1}H NMR-titration experiments are performed in DMSO-d$_6$ to elucidate the binding mode of ligand H$_2$L with Zn^{2+} in solution. All aromatic and aliphatic protons of the ligand H$_2$L are shifted towards upfield due to complexation with Zn^{2+} (Figure 16).

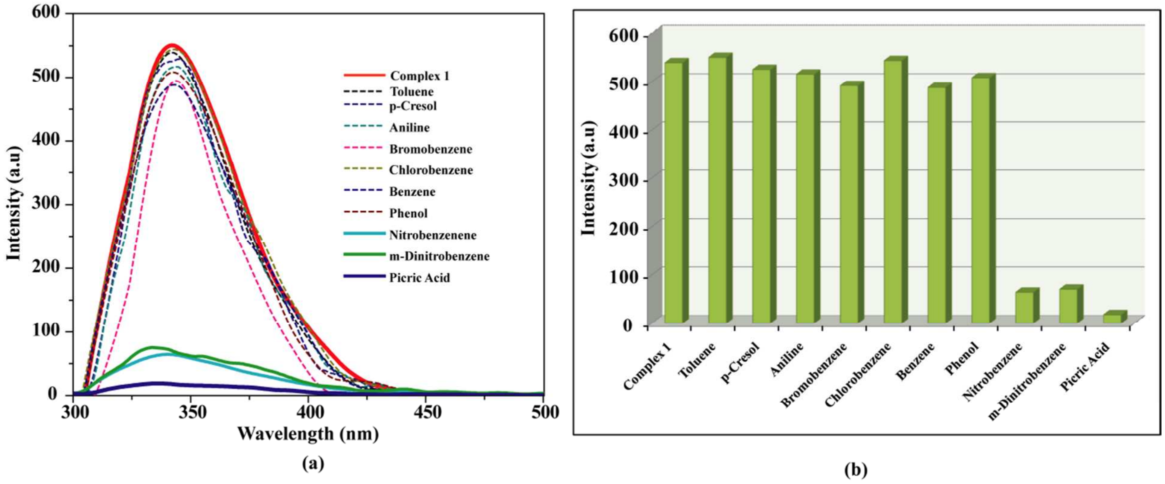

Figure 17: (a) Fluorescence spectra of complex **1** in methanol (excitation wavelength 290 nm and conc. 10^{-5} M) upon the addition of various organic analytes (5.0 equivalent). (b) Relative changes in fluorescent intensity of complex **1** in presence of different organic analytes (5.0 equivalent).

Nitro sensing

In order to explore the potential application of zinc complexes as sensors for hazardous organic analytes, fluorescence spectra of complexes **1-3** are recorded in presence of various organic analytes such as benzene, chlorobenzene, bromobenzene, phenol, aniline, xylene, p-cresol and aromatic nitro compounds. But significant quenching of fluorescence intensity is observed only upon addition of nitroaromatics such as nitrobenzene, nitrotoluene, nitrophenol, DNT, picric acid(PA) etc. (figure 17). This observation reveals that zinc complexes **1-3** can be used as potential sensors for selective detection of nitroaromatics. The reason for the significantly high quenching of fluorescence intensity by nitroaromatics compared to other aromatics is most likely due to their more electron deficient nature. The substantial quenching of fluorescence intensity is observed upon addition of PA in comparison to other nitroaromatics. So, we have performed fluorescence titration of zinc complexes (**1-3**) in methanol by the addition of PA with gradual increase in concentration. The fluorescence intensity of complex **1** kept on decreasing with an increase in the concentration of PA is shown in figure 18 (for complexes **2** and **3** figures S11 and S12, Supporting Information). The efficient quenching of PA in this system can be explain to the polarizability of PA in methanol and also the π–π interaction between analytes and the host materials, which induces the electron transfer from the excited zinc complex to electron-deficient PA.[73,74]

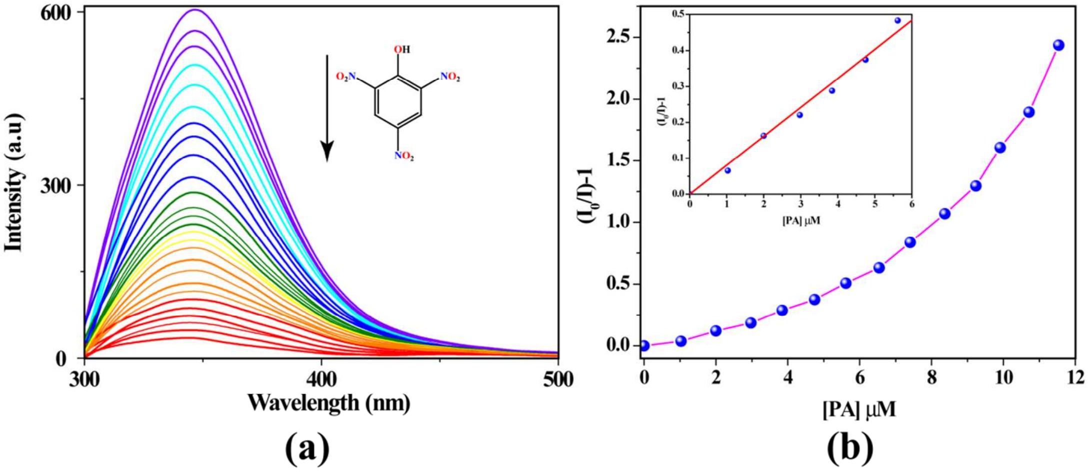

Figure 18: (a) Fluorescence spectra of complex **1** in methanol methanol (excitation wavelength 290 nm and conc. 10^{-5} M) upon increasing concentration of PA. (b) Stern−Volmer plot of complex **1**.

The quenching efficiency of PA is quantitatively determined by the Stern-Volmer equation (Equation 6, Supporting information).[72]At low concentrations, the Stern-Volmer plot of PA is linear where as at higher concentrations, consequently deviate from linearity and turn upward (figure 18b), which may be due to self-absorption.[75-77] The Stern-Volmer quenching constants (K_{sv}) is calculated from the slope of the linearly fitted curve (figure 18b) is 8.063 × 10^4 M^{-1} ($R^2 = 0.994$) for complex **1** (for complexes **2** and **3**, K_{sv} are 7.987 × 10^4 M^{-1} ($R^2 = 0.998$) and 8.51 × 10^4 M^{-1} ($R^2 = 0.999$) respectively, figures S11 and S12, Supporting Information), which is comparatively higher than those reported other fluorescence chemosensors for PA.[78-81]

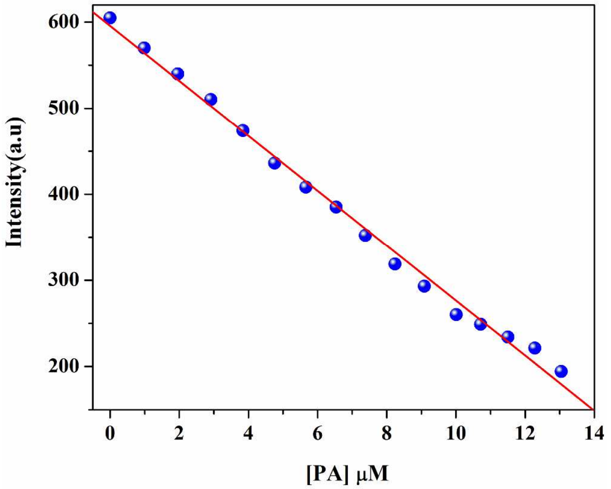

Figure 19: Plot of limit of detection of complex **1** towards PA.

The limit of detection of PA is 3.986 × 10^{-9} M (912 ppt) calculated from figure 19 for complex **1** (for complexes **2** and **3**, LOD are 3.974 × 10^{-9} M (910 ppt) and 3.914 × 10^{-9} M (896 ppt) respectively, figures S13 and S14, Supporting Information). To the best of our knowledge, this is the lowest detectable concentration of Picric Acid among the reported chemosensor for selective sensing of PA till date.[82-85]

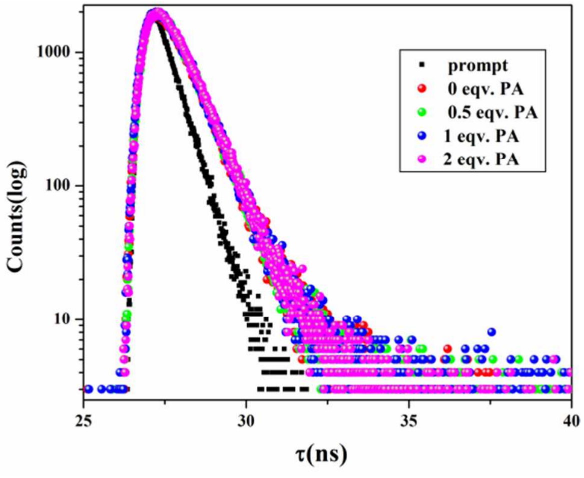

Figure 20: Fluorescence decay profile of complex **1** with different amount of PA.

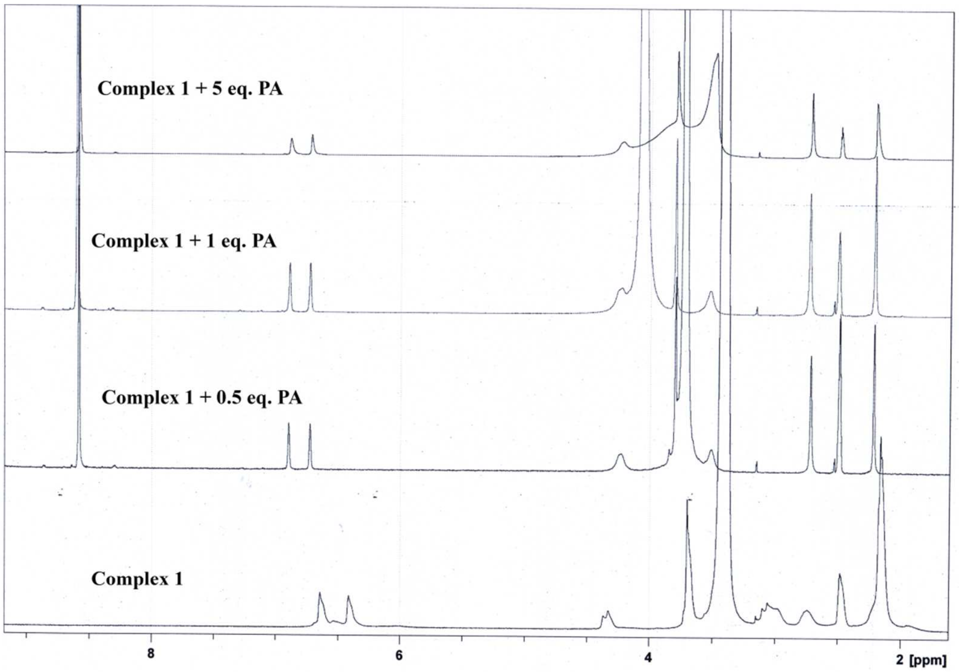

Figure 21: ^{1}HNMR titration of complex **1** with varying amount of PA in DMSO-d$_6$.

The fluorescence lifetime of complex **1** is measured in presence of different concentration of PA to check the existence of dynamic quenching but observed no change in excited state lifetime (figure 20), which implied that the quenching pathway is static only. In order to find out the binding mechanism of PA with complex **1** in solution we have perform ^{1}HNMR titration with varying the amount of PA (0, 0.5, 1 and 5 equivalent) in DMSO-d$_6$ (figure 21).

We observed that all protons are shifted to downfield region that means PA withdrawn electron density from complex **1** and shifted proton towards deshielded region. By comparing the ^{1}HNMR titration spectra (Figures 16 and 21) it is clear that no ligand substitution is observed during the interaction of PA with complex **1** which is again confirm by mass spectrometry data for this titration (Figure S15, Supporting Information). From the mass spectrometry data it is seen that a dinuclear ternary complex is form with PA $[Zn_2L(PA)]^+$ shows a base peak at m/z 744.06 (calcd 744.07).

Conclusions

In order to rationalize the coordination behavior of the flexidentate polytopic Mannich base ligand, H_2L towards metal ion that determine the nuclearity of the resulting complexes, we have prepared three Zn(II) and three Cd(II) complexes varying the anionic co-ligands under similar reaction conditions. All three complexes of Zn(II) are dinuclear and the coordination mode of the ligand is hexa- or heptadentate, both of which can be explained considering the preference of Zn(II) for lower coordination number (four or five). On the other hand, preference for higher coordination (six or seven) number of Cd(II) makes the ligand octa-dentate in its all three complexes and consequently tetranuclear complexes are formed that get additional stability with the help of respective μ_3-bridging anionic co-ligands (azide, acetate or chloride). The polytopic Manich base ligand H_2L is found to be very efficient in acting as potential luminiscence sensor for the selective detection of Zn(II) ion. The detection limit of Zn^{2+} ion is 7.69 nM, which is higher than most of the reported fluorescence sensors for Zn^{2+} ion with binding constant $K=1.508 \times 10^{10}$ M^{-2}. The produced Zn(II) complexes can also be used as sensor for the selective detection of nitroaromatic explosives The solution phase sensing mechanism has been studied thoroughly. The detection limit of PA has been found to be the lowest (in ppt level) among all the reported complexes. Thus, the synthetic simplicity, cost-effectiveness and high sensitivity of the Zn(II) complexes are expected to make them useful as sensor for picric acid.

Supporting Information

CCDC reference numbers are **1569928-1569933** for complexes **1-6** respectively, contain supplementary crystallographic data for this paper. These data can be obtained free of charge from The Cambridge Crystallographic Data Centre via www.ccdc.cam.ac.uk/data_request/cif.

ORTEP diagram of complex 6B, selected bond lengths and angles of all complexes, geometrical features of hydrogen bonding interactions and crystallographic data for complexes **1-6**, Mass and NMR spectra of ligand and complexes **1**-**3**, Fluorescence spectra, Stern−Volmer plot and LOD calculation of complexes **2** and **3** in methanol upon increasing concentration of PA.

Acknowledgements

A. Das and S. Jana are thankful to the University Grants Commission (UGC), New Delhi, for Senior Research Fellowship [Sanction No. UGC/1253/JR. Fellow (Sc)] and Dr. D. S. Kothari Postdoctoral Fellowship [Award letter no.F.4-2/2006(BSR)/CH/15-16/0121] respectively.

Table 1: Crystal data and structure refinement of complexes **1-6.**

Complex	**1**	**2**	**3**	**4**	**5**	**6**
Formula	$C_{22}H_3Cl_2N_2Zn_2O_5$	$C_{24}H_{32}N_4Zn_2O_6S_2$	$C_{24}H_{33}N_5Zn_2O_6$	$C_{44}H_{60}Cd_4Cl_4N_4O_9$	$C_{50}H_{66}Cd_4N_6O_{14}S_2$	$C_{48}H_{66}Cd_4N_{10}O_{15}$
Formula weight	606.18	667.46	618.33	1380.40	1488.85	1472.75
Temp (K)	293	293	293	293	293	293
Crystal System	Monoclinic	Monoclinic	Monoclinic	Monoclinic	Monoclinic	Monoclinic
Space group	*P*21/*c*	*P*21/*c*	*P*21/*n*	*P*21	*P*21/*n*	*P*21/*c*
a/Å	17.4024(11)	17.9488(14)	11.2371(8)	10.9102(5)	11.038(3)	22.6091(16)
b/Å	13.3329(8)	12.3478(9)	14.5967(11)	20.3214(8)	18.718(4)	12.3306(9)
c/Å	11.0429(7)	14.8452(11)	16.5066(12)	11.6017(5)	29.734(7)	21.6595(15)
β/°	95.699(2)	105.256(3)	95.170(3)	96.697(1)	94.577(3)	98.459(3)
Z	4	4	4	2	4	4
D_c/g cm^{-3}	1.579	1.397	1.523	1.794	1.615	1.638
μ/mm^{-1}	2.126	1.683	1.826	1.906	1.501	1.473
F (000)	1248	1376	1280	1368	2976	2944
R(int)	0.058	0.061	0.082	0.041	0.055	0.031
Total Reflections	42797	52715	54413	62861	27155	149435
Unique reflections	4538	5656	4767	9029	10032	10681
Observed data $I>2\sigma(I)$	4004	4884	3824	8839	7424	9467
R1, *w*R2(all data)	0.0373, 0.0800	0.0707, 0.2026	0.0430, 0.1101	0.0223, 0.0565	0.0724, 0.1671	0.0535, 0.1344
R1, *w*R2 $[I>2\sigma(I)]$	0.0308, 0.0769	0.0824, 0.2104	0.0612, 0.1256	0.0215, 0.0558	0.0510, 0.1520	0.0453, 0.1266
GOF on F^2	1.077	1.476	1.107	1.168	1.049	1.192

Table 2: Fluorescence life time data of H_2L and complexes **1-3**.

	α_1(%)	**τ_1(ns)**	**α_2(%)**	**τ_2(ns)**	**τ_{av}(ns)**	**χ^2**
H_2L	54.68	0.404	45.32	1.14	0.919	1.019
1	87	0.439	13	1.25	0.682	1.037
2	76.32	0.490	23.68	0.973	0.674	1.023
3	91.75	0.659	8.25	0.156	0.817	0.986

References

(1) Riddel, I. A.; Hristova, Y. R.; Clegg, J. K.; Wood, C. S.; Breiner, B.; Nitschke, J. K. Five Discrete Multinuclear Metal-Organic Assemblies from One Ligand: Deciphering the Effects of Different Templates. *J. Am. Chem. Soc*. **2013**, *135*, 2723−2733.

(2) Ahmed, B. M.; Mezei, G. Accessing the inaccessible: discrete multinuclear coordination complexes and selective anion binding attainable only by tethering ligands together. *Chem. Commun.* **2017**, *53*, 1029−1032.

(3) Barnett, S. A.; Champness N. R. Structural diversity of building-blocks in coordination framework synthesis combining M$(NO_3)_2$ junctions and bipyridyl ligands. *Coord. Chem. Rev.* **2003**, *246*, 145–168.

(4) Jana, S.; Harms, K.; Bauzá, A.; Frontera, A.; Chattopadhyay, S. Synthesis, Structures, and DFT Study of CuBr Based Coordination Polymers via in Situ Reduction of Copper(II). *Cryst. Growth Des*. **2015**, *15*, 257−267.

(5) Mahapatra, P.; Drew, M. G. B.; Ghosh, A. Variations of Structures and Phenoxazinone Synthase-like Activity of the Complexes Based on $(Cu^{II})_2Mn^{II}$ Node and Dicyanamide Spacer. *Cryst. Growth Des*. **2017**, *17*, 6809−6820.

(6) Ghosh, S.; Ida Y.; Ishida, T.; Ghosh, A. Linker Stoichiometry-Controlled Stepwise Supramolecular Growth of a Flexible Cu_2Tb Single Molecule Magnet from Monomer to Dimer to One-Dimensional Chain. *Cryst. Growth Des*. **2014**, *14*, 2588−2598.

(7) Sheikh, J. A.; Jena, H. S.; Clearfield, A.; Konar, S. Phosphonate Based High Nuclearity Magnetic Cages. *Acc. Chem. Res.* **2016**, *49*, 1093−1103.

(8) Mahapatra, P.; Ghosh, S.; Giri, S.; Rane, V.; Kadam, R.; Drew, M. G. B.; Ghosh, A. Subtle Structural Changes in $(Cu^{II}L)_2Mn^{II}$ Complexes To Induce Heterometallic Cooperative Catalytic Oxidase Activities on Phenolic Substrates (H_2L = Salen Type Unsymmetrical Schiff Base). *Inorg. Chem*. **2017**, *56*, 5105−5121.

(9) Pârvulescu, A. N.; Marin, G.; Suwinska, K.; Kravtsov, V. C.; Andruh, M.; Pârvulescu, V.; Pârvulescu, V. I. A polynuclear complex, $\{[Cu(bpe)_2](NO_3)\}$, with interpenetrated diamondoid networks: synthesis, properties and catalytic behaviour. *J. Mater. Chem.* **2005**, *15*, 4234–4240.

(10) Brzostek, K. S.; Terlecki, M.; Sokołowski, K.; Lewinski, J. Chemical fixation and conversion of CO2 into cyclic and cage-type metal carbonates, *Coordination Chemistry Reviews*. **2017**, *334*, 199–231.

(11) Li, X.; Wu, B. L.; Niu, C. Y.; Niu, Y. Y.; Zhang, H. Y. Syntheses of Metal-2-(Pyridin-4-yl)-1H-imidazole-4,5-dicarboxylate Networks with Topological Diversity: Gas Adsorption, Thermal Stability and Fluorescent Emission Properties. *Cryst. Growth Des*. **2009**, *9*, 3423−3431.

(12) Chen, M.; Chen, S. S.; Okamura, T.; Su, Z.; Chen, M. S.; Zhao, Y.; Sun, W. Y.; Ueyama, N. pH Dependent Structural Diversity of Metal Complexes with 5-(4H-1,2,4-Triazol-4-yl)benzene-1,3-dicarboxylic Acid, Cryst. Growth Des. **2011**, *11*, 1901–1912.

(13) Das, L. K.; Ghosh, A. Structural diversity in the complexes based on a hetero-trimetallic Cu2Cd node and dicyanamide spacer: a hexanuclear cluster, a 1D stair polymer and a 1D zigzag chain as supramolecular isomers, and a 3D network. *CrystEngComm*. **2013**, *15*, 9444-9456.

(14) Han, Y.; Zhang, Z.; Liu, Y.; Niu, Y.; Ding, D.; Wu, B.; Hou, H.; Fan, Y. External emplate-Assisted Self-Assembly:Design and Synthesis of 4,4′-bipy-Based Mo(W)/Cu/S Heterothiometallic Polymeric Clusters Directed by 1,10-Bis(pyridinium)methylene Cation. Cryst. Growth Des. **2011**, *11,* 3448–3455.

(15) Zheng, B.; Dong, H.; Bai, J.; Li, Y.; Li, S.; Scheer, M. Temperature Controlled Reversible Change of the Coordination Modes of the Highly Symmetrical Multitopic Ligand To Construct Coordination Assemblies:Experimental and Theoretical Studies. *J. Am Chem. Soc.* **2008**, *130*, 7778–7779.

(16) Botana, L.; Ruiz, J.; Seco, J. M.; Mota, A. J.; Dieguez, A. R.; Sillanpaa R.; Colacio, E. Influence of the anions on the structure and magnetic properties of a series of bis(l-diphenoxo)-bridged linear trinuclear copper(II) complexes: an experimental and theoretical study. *Dalton Trans*., **2011**, *40*, 12462–12471.

(17) Xie, Q. W.; Wu, S. Q.; Liu, C. M.; Cuia, A. L.; Kou, H. Z. Synthesis, crystal structure and magnetic properties of dinuclear $Ni^{II}Ln^{III}$ complexes based on a flexible polydentate ligand. *Dalton Trans.,* **2013**, *42*, 11227–11233.

(18) Xie, Q. W.; Wu, S. Q.; Shi, W. B.; Liu, C. M.; Cuia, A. L.; Kou, H. Z. Heterodinuclear M(II)–Ln(III) single molecule magnets constructed from exchange-coupled single ion magnets. *Dalton Trans*. **2014**, *43*, 11309–11316.

(19) Botana, L.; Ruiz, J.; Mota, A. J.; Dieguez, A. R.; Seco, J. M.; Oyarzabala, I.; Colacio, E. Anion controlled structural and magnetic diversity in unusual mixed-bridged polynuclear Ni(II) complexes with a versatile bis(2-methoxy phenol)diamine hexadentate ligand. An experimental and theoretical magneto-structural study. *Dalton Trans.* **2014**, *43*, 13509–13524.

(20) Asthana, S. K.; Kumar, A.; Neeraj; Shweta; Hira, S. K.; Manna, P. P. Brightening Quinolineimines by Al^{3+} and Subsequent Quenching by PPi/PA in Aqueous Medium: Synthesis, Crystal Structures, Binding Behavior, Theoretical and Cell Imaging Studies. *Inorg. Chem*. **2017**, *56*, 3315−3323.

(21) Yao, P. S.; Liu, Z.; Ge, J. Z.; Chenb, Y.; Cao, Q. Y. A novel polynorbornene-based chemosensor for the fluorescence sensing of Zn^{2+} and Cd^{2+} and subsequent detection of pyrophosphate in aqueous solutions. *Dalton Trans*. **2015**, *44*, 7470–7476.

(22) Hu, Z.; Deibert, B. J.; Li, J. Luminescent metal–organic frameworks for chemical sensing and explosive detection. *Chem. Soc. Rev*. **2014**, *43*, 5815 −5840.

(23) Gale, P. A.; Caltagirone, C. Anion sensing by small molecules and molecular ensembles. *Chem. Soc. Rev.,* **2015**, *44*, 4212—4227.

(24) Chen, B.; Wang, L.; Zapata, F.; Qian, G.; Lobkovsky, E. B. A Luminescent Microporous Metal-Organic Framework for the Recognition and Sensing of Anions. *J. Am. Chem. Soc.* **2008**, *130*, 6718–6719.

(25) Suresh, V. M.; Bandyopadhyay, A.; Roy, S.; Pati, S. K.; Maji, T. K. Highly Luminescent Microporous Organic Polymer with Lewis acidic 'Boron' Sites on the Pore Surface: Ratiometric Sensing and Capture of F^- Ion. *Chem. Eur. J.* **2015,** *21*, 10799 –10804.

(26) Moradpour, T.; Abbasi, A.; Hecke, K. V. A nanoporous 3D zinc(II) metal–organic frame work for selective absorption of benzaldehyde and formaldehyde. *Journal of Solid State Chemistry*, **2015**, *228*, 36–41.

(27) Hu, Z.; Deibert, B. J.; Li, J. Luminescent metal–organic frameworks for chemical sensing and explosive detection, *Chem. Soc. Rev*., **2014**, *43*, 5815−5840.

(28) Wang, D.; Zhang, L.; Li, G.; Huo, Q.; Liu, Y. Luminescent MOF material based on cadmium(II) and mixed ligands: application for sensing volatile organic solvent molecules. *RSC Adv*. **2015**, *5*, 18087–18091.

(29) Acharyya, K.; Mukherjee, P. S. A fluorescent organic cage for picric acid detection. *Chem. Commun*. **2014**, *50*, 15788-15791.

(30) Berg, J. M.; Shi, Y. The Galvanization of Biology: A Growing Appreciation for the Roles of Zinc, Science. **1996**, *271*,1081-1085.

(31) Vallee, B. L.; Falchuk, K. H. The Biochemical Basis of Zinc Physiology, *Physiological Reviews*. **1993**, *73*, 79-105.

(32) Satarug, S.; Baker, J. R.; Urbenjapol, S.; Elkins, M. H.; Reilly, P. E. B.; Williams, D. J.; Moore, M. R. A global perspective on cadmium pollution and toxicity in non-occupationally exposed population, *Toxicology Letters*, 2003,*137*, 65–83.

(33) Liu, L.; Ding, J.; Huang, C.; Li, M.; Hou, H.; Fan, Y. Polynuclear Cd(II) Polymers:Crystal Structures, Topologies, and the Photodegradation for Organic Dye Contaminants. *Cryst. Growth Des*. **2014**, *14*, 3035−3043.

(34) Kumar, R.; Bhargava, P.; Chauhan, G.; Srivastava, R. Synthesis and Characterization of Cadmium Complex and Its Application in Organic Light Emitting Diodes(OLEDs). *Advanced Science Letters.* **2014**, *20*, 1001−1004.

(35) He, H.; Song, Y.; Sun, F.; Zhao, N.; Zhu,G. Sorption Properties and Nitroaromatic Explosives Sensing Based on Two Isostructural Metal‒Organic Frameworks. *Cryst. Growth Des*. **2015**, *15*, 2033‒2038.

(36) Santra, P. K.; Kamat, P. V. Tandem-Layered Quantum Dot Solar Cells: Tuning the Photovoltaic Response with Luminescent Ternary Cadmium Chalcogenides. *J. Am. Chem. Soc.* **2013**, *135*, 877‒885.

(37) Roy, S.; Dey, A. Ray, P. P.; Castro,J. O.; Frontera, A.; Chattopadhyay, S. Application of a novel 2D cadmium(II)-MOF in the formation of a photo-switch with a substantial on–off ratio, *Chem. Commun.,* **2015**, *51*, 12974–12976.

(38) Liu, L. L.; Yu, C. X.; Du, J. M.; Liu, S. M.; Caoa, J. S.; Ma, L. F. Construction of five Zn(II)/Cd(II) coordination polymers derived from a new linear carboxylate/pyridyl ligand: design, synthesis, and photocatalytic properties. *Dalton Trans*., **2016**, *45*, 12352–12361.

(39) Roy, S.; Harms, K.; Bauzá, A.; Frontera, A.; Chattopadhyay, S. Exploration of photocatalytic activity of an end-on azide bridged one-dimensional cadmium(II) Schiff base complex for the degradation of organic dye in visible light. *Polyhedron.* **2017**, *121*, 199–205.

(40) Liu, X.; Wang, P.; Fu, J.; Yao, K.; Xue, K.; Xu, K. Turn-on fluorescent sensor for Zinc and Cadmium ions based on quinolone and its sequential response to phosphate. *Journal of Luminescence*. **2017**, *186*,16–22.

(41) Yao, P. S.; Liu, Z.; Ge, J. Z.; Chenb, Y.; Cao, Q. Y. A novel polynorbornene-based chemosensor for the fluorescence sensing of Zn^{2+} and Cd^{2+} and subsequent detection of pyrophosphate in aqueous solutions. *Dalton Trans*. **2015**, *44*, 7470–7476.

(42) Singh, R.; Gogoi, A.; Das, G. Benzothiazole based multi-analyte sensor for selective sensing of Zn^{2+} and Cd^{2+} and subsequent sensing of inorganic phosphates (Pi) in mixed aqueous medium. *RSC Adv.* **2016**, *6*, 112246-112252.

(43) Lim, N. C.; Schuster, J. V.; Porto, M. C.; Tanudra, M. A.; Yao, L.; Freake, H. C.; Bruckner, C. Coumarin-Based Chemosensors for Zinc(II): Toward the Determination of the Design Algorithm for CHEF-Type and Ratiometric Probes. *Inorganic Chemistry.* **2005**, *44*, 2018‒2030.

(44) Lee, J. J.; Lee, S. A.; Kim, H.; Nguen, L.; Noh, I.; Kim, C. A highly selective CHEF-type chemosensor for monitoring Zn^{2+} in aqueous solution and living cells. *RSC Adv.,* **2015,** *5,* 41905-41913.

(45) Ganguly, A.; Ghosh, S.; Kar, S.; Guchhait, N. Selective fluorescence sensing of Cu(II) and Zn(II) using a simple Schiff base ligand: Naked eye detection and elucidation of photoinduced electron transfer (PET) mechanism, *Molecular and Biomolecular Spectroscopy.* **2015**, *143*, 72‒80.

(46) Choi, M.; Kim, M.; Lee, K. D.; Han, K. N.; Yoon, I. A.; Chung, H. J.; Yoon, J. A New Reverse PET Chemosensor and Its Chelatoselective Aromatic Cadmiation. *Org. Lett.* **2001**, *3,* 3455–3457.

(47) Wang, W.; Yang, J.; Wang, R.; Zhang, L.; Yu, J.; Sun, D. Luminescent Terbium-Organic Framework Exhibiting Selective Sensing of Nitroaromatic Compounds (NACs). *Cryst. Growth Des*. **2015**, *15*, 2589−2592.

(48) Salinas, Y.; Manez, R. M.; Marcos, M. D.; Sancenon, F. L.; Costero, A. M.; Parra, M.; Gil, S. Optical chemosensors and reagents to detect explosives. *Chem. Soc. Rev*. **2012**, *41*, 1261–1296.

(49) Steinfeld, J. I.; Wormhoudt, J. Explosives detection: A Challenge for Physical Chemistry. *Annu. Rev. Phys. Chem*. **1998**. *49*, 203–232.

(50) Caygill, J. S.; Davis, F.; Higson, S. P. J. Current trends in explosive detection techniques. *Talanta.* **2012,** *88*, 14–29.

(51) Czarnik, A. W. A sense for landmines. *Nature.* **1998**, *394*, 417–418.

(52) Chowdhury, A.; Mukherjee, P. S. Vinylanthracene-Based Compounds as Electron-Rich Sensors for Explosives Recognition. *ChemPlusChem***.** **2016**, *81,* 1360–1370.

(53) Toal, S. J.; Trogler,W. C. Polymer sensors for nitroaromatic explosives detection. *J. Mater. Chem.*, **2006**, *16*, 2871–2883.

(54) Banerjee, D.; Hu, Z.; Pramanik, S.; Zhang, X.; Wang, H.; Li, J. Vapor phase detection of nitroaromatic and nitroaliphatic explosives by fluorescence active metal‑organic frameworks. *CrystEngComm*. **2013**, *15*, 9745‑9750.

(55) Sheldrick, G. M. A short history of SHELX. *Acta Crystallogr.* **2008**, *A64*,112-122.

(56) Sheldrick, G. M. SADABS: Software for Empirical Absorption Correction, University of Gottingen, Institute fur Anorganische Chemieder Universitat, Gottingen, Germany, 1999-2003.

(57) Das, A.; Bhattacharya, K.; Giri, S.; Ghosh, A. Synthesis, crystal structure and magnetic properties of a dinuclear and a trinuclear Ni(II) complexes derived from tetradentate ONNO donor Mannich base ligands. *Polyhedron*. **2017**, *134,* 295–301.

(58) Ghosh, S.; Aromí, G.; Gamez, P.; Ghosh, A. The Impact of Anion-Modulated Structural Variations on the Magnetic Coupling in Trinuclear Heterometallic $\mathrm{Cu^{II}}$–$\mathrm{Co^{II}}$ Complexes Derived from a Salen-Type Schiff Base Ligand. *Eur. J. Inorg. Chem.* **2014**, 3341-3349.

(59) Addison, A. W.; Rao, T. N.; Reedijk, J.; Rijn, J. V.; Verschoor, G. C. Synthesis, structure, and spectroscopic properties of copper(II) compounds containing nitrogen−sulphur donor ligands; the crystal and molecular structure of aqua[1,7-bis(N-methylbenzimidazol-2-yl)-2,6-dithiaheptane]copper(II) perchlorate. *J. Chem. Soc., Dalton Trans.* **1984**, 1349−1356.

(60) Roy, S.; Bhaumik, P. K.; Harms, K.; Chattopadhyay, S. Synthesis and characterization of three new photo-luminescent cadmium(II) complexes with azide: Variation in molecular structures with changes in the denticity of blocking ligands. *Inorganica Chimica Acta.* **2015**, *427*, 155–161.

(61) Ako, A. M.; Burger, B.; Lan, Y.; Mereacre, V.; Clérac, R.; Buth, G.; Coca, S. G.; Ruiz, E.; Anson, C. E.; Powell, A. K. Magnetic Interactions Mediated by Diamagnetic Cations in [$Mn_{18}M$] (M = Sr^{2+}, Y^{3+}, Cd^{2+}, and Lu^{3+}) Coordination Clusters. *Inorg. Chem.* **2013**, *52,* 5764 −5774.

(62) Bai, S. Q.; Fang, C. J.; He, Z.; Gao, E. Q.; Yan, C. H.; Hor, T. S. A. Azide-bridged Cd(II) 1D coordination polymer with Cd_{13} nano-crown-like cluster. *CrystEngComm*. **2013**, *15*, 650–653.

(63) Machura, B.; Nawrot, I.; Michalik, K. Synthesis, spectroscopic characterization and X-ray studies of two novel double open cubane-like cadmium(II) complexes. *Polyhedron.* **2012**, *31* 548–557.

(64) Mikata, Y.; Ohnishi, R.; Nishijima, R.; Konno, H. Fluorescent Detection of Phosphate Ion via a Tetranuclear Zinc Complex Supported by a Tetrakisquinoline Ligand and μ_4-PO_4 Core. *Inorg. Chem.* **2016**, *55*, 11440−11446.

(65) Parmar, B.; Rachuri, Y.; Bisht, K. K.; Laiya, R.; Suresh, E.; Mechanochemical and Conventional Synthesis of Zn(II)/Cd(II) Luminescent Coordination Polymers: Dual Sensing Probe for Selective Detection of Chromate Anions and TNP in Aqueous Phase. *Inorg. Chem.* **2017**, *56*, 2627−2638.

(66) Wang, D.; Li, S.-M.; Zheng, J.-Q.; Kong, D.-Y.; Zheng, X.-J.; Fang, D.-C.; Jin, L.-P. Coordination-Directed Stacking and Aggregation-Induced Emission Enhancement of the Zn(II) Schiff Base Complex. *Inorg. Chem.* **2017**, *56*, 984−990.

(67) Carlosa, F. d. S.; Nunesa, M. C.; Bonib, L. D.; Machadoc, G. S.; Nunesa, F. S. A novel fluorene-derivative Schiff-base fluorescent sensor for copper (II) in organic media. *Journal of Photochemistry and Photobiology A: Chemistry*. **2017**, *348*, 41–46.

(68) Wang, D.; Li, S.-M.; Zheng, J.-Q.; Kong, D.-Y.; Zheng, X.-J.; Fang, D.-C.; Jin, L.-P. Coordination-Directed Stacking and Aggregation-Induced Emission Enhancement of the Zn(II) Schiff Base Complex. Inorg. Chem. 2017, 56, 984−990.

(69) Jisha, V. S.; Thomas, A. J.; Ramaiah, D. Fluorescence Ratiometric Selective Recognition of Cu^{2+} Ions by Dansyl−Naphthalimide Dyads. J. Org. Chem. 2009, 74, 6667−6673.

(70) Yang, R.; Li, K.; Wang, K.; Zhao, F.; Li, N.; Liu, F. Porphyrin Assembly on β-Cyclodextrin for Selective Sensing and Detection of a Zinc Ion Based on the Dual Emission Fluorescence Ratio. Anal. Chem. 2003, 75, 612−621.

(71)Jana, S.; Chattopadhyay, S. Design and construction of copper(I) complexes based on flexi-dentate cyclic N_2-donor Schiff bases via in situ reduction of copper(II) precursors. *Polyhedron*. **2014**, *81*, 298–307.

(72) Sinha, S.; Chowdhury, B.; Ghosh, P. A Highly Sensitive ESIPT-Based Ratiometric Fluorescence Sensor for Selective Detection of Al^{3+}. *Inorg. Chem*. **2016**, *55*, 9212−9220.

(73) Sun, L.; Xing, H.; Xu, J.; Liang, Z.; Yua, J.; Xua, R. A novel (3,3,6)-connected luminescent metal–organic framework for sensing of nitroaromatic explosives. *Dalton Trans*. **2013**, *42*, 5508–5513.

(74) Barman, S.; Garg, J. A.; Blacque, O.; Venkatesan, K.; Berke, H. Triptycene based luminescent metal–organic gels for chemosensing. *Chem. Commun.* **2012**, *48*, 11127–11129.

(75) Wang, Z.J.; Qin, L.; Chen, J. Xi.; Zheng, H.G. H‑Bonding Interactions Induced Two Isostructural Cd(II) Metal−Organic Frameworks Showing Different Selective Detection of Nitroaromatic Explosives. *Inorg. Chem.* **2016**, *55*, 10999−11005.

(76) Lan, A.; Li, K.; Wu, H.; Olson, D. H.; Emge, T. J.; Ki, W.; Hong, M.; Li, J. A Luminescent Microporous Metal−Organic Framework for the Fast and Reversible Detection of High Explosives. *Angew. Chem. Int. Ed*. **2009**, *48*, 2334−2338.

(77) Gole, B.; Shanmugaraju, S.; Bar, A. K.; Mukherjee, P. S. Supra molecular polymer for explosives sensing: role of H-bonding in enhancement of sensitivity in the solid state. *Chem. Commun.* **2011**, *47*, 10046–10048.

(78) Liu, C. L.; Zhou, L.P.; Tripathy, D.; Sun, Q. F. Self-assembly of stable luminescent lanthanide supramolecular M_4L_6 cages with sensing properties toward nitroaromatics. *Chem. Commun*. **2017**, *53*, 2459–2462.

(79) Nagendran, S.; Vishnoi, P.; Murugavel, R. Triphenylbenzene Sensor for Selective Detection of Picric Acid. *J Fluoresc*. **2017**, *27*, 1299–1305.

(80) Sahoo, J.; lakshmi, D. S.; Suresh, E.; Subramanian, P.S. Selective and sensitive detection of picric acid in aqueous, sol-gel and solid support media by Ln(III) probes. *Sensors and Actuators B*. **2017**, *250,* 215–223.

(81) Fu, R.; Hu, S.; Wu, X. Luminescent Zinc Phosphonates for Ratiometric Sensing of 2,4,6-Trinitrophenol and Temperature. *Cryst. Growth Des*. **2016**, *16*, 5074−5083

(82) Shanmugaraju, S.; Dabadie, C.; Byrne, K.; Savyasachi, A. J.; Umadevi, D.; Schmitt, W.; Kitchen, J. A.; Gunnlaugsson, T. A supramolecular Tr¨oger's base derived coordination zinc polymer for fluorescent sensing of phenolic-nitroaromatic explosives in water. *Chem. Sci.,* **2017**, *8*, 1535−1546.

(83) Li, X. Z.; Zhou, L.P.; Yan, L.L.; Yuan, D. Q.; Lin, C. S.; Sun, Q. F. Evolution of Luminescent Supramolecular Lanthanide $M_{2n}L_{3n}$Complexes from Helicates and Tetrahedra to Cubes. *J. Am. Chem. Soc.,* **2017**, *139*, 8237−8244.

(84) Santra, D. C.; Bera, M. K.; Sukul, P. K.; Malik, S. Charge-Transfer-Induced Fluorescence Quenching of Anthracene Derivatives and Selective Detection of Picric Acid. *Chem. Eur. J.,* **2016**, *22*, 2012 – 2019.

(85) Swamy P, C. A.; Thilagar, P. Polyfunctional Lewis Acids: Intriguing Solid-State Structure and Selective Detection and Discrimination of Nitroaromatic Explosives. *Chem. Eur. J.,* **2015**, *21*, 8874 – 8882.

For Table of Contents Use Only

Modulation of nuclearity by Zn(II) and Cd(II) in their complexes with a polytopic Mannich base ligand: a turn-on luminescence sensor for Zn(II) and detection of nitroaromatic explosives by the Zn(II) complexes

Avijit Das, Subrata Jana, Ashutosh Ghosh*

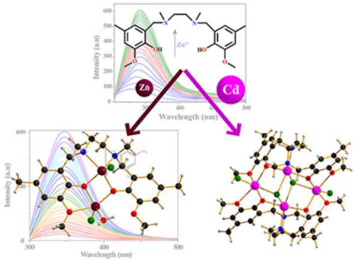

Reactions of Zn^{II} ion with the ligand H_2L in presence of bridging co-ligands, yielded three new dinuclear complexes, whereas Cd^{II} ion formed three new tetranuclear complexes, with the same ligand and co-ligands. The ligand, H_2L exhibited highly selective turn-on fluorescence sensing property for Zn^{2+} ion. All three Zn^{II} complexes also show fluorescence and can be used as florescence sensors for specific recognition of nitroaromatic explosives.